

Aggregated spots and waving loops in a reaction-advection-diffusion system with a global coupling

Yasuaki Kobayashi* and Masaki Sano

Department of Physics, The University of Tokyo, Hongo, Tokyo 113-0033, Japan

(Received 15 April 2005; published 26 January 2006)

We construct a phenomenological model describing aggregated spots and a loop structure. Our model is based on the Gray-Scott model which is supplemented with a global coupling term and advection terms. One of the species makes a field proportional to its concentration, which induces the advection. By numerically investigating the model, we show that the system has a transition from aggregated spots to a loop which wanders around chaotically or reaches a stationary state. Relation to a similar transition observed in a recent gas discharge experiment [S. Nasuno, *Chaos* **13**, 3 (2003)] is discussed.

DOI: [10.1103/PhysRevE.73.015104](https://doi.org/10.1103/PhysRevE.73.015104)

PACS number(s): 82.40.Ck, 47.54.-r, 89.75.Kd, 05.65.+b

Localized structures are one of the most remarkable features in the systems driven out of equilibrium such as granular systems [1], convection of a nematic liquid crystal [2], binary liquid convection [3], and vibrated fluid systems [4]. Complex structures such as a cluster of spots have also been observed in gas-discharge systems [5,6] and nonlinear optics [7]. Models based on reaction-diffusion systems have been proposed [6,8] and they can successfully describe such localized clusters.

The purpose of this paper is to propose a model which can produce localized structures. The model is a variant of the Gray-Scott model [9], which is supplemented with advective terms and a global coupling. The governing equations are as follows:

$$\frac{\partial u}{\partial t} + \vec{\nabla} \cdot (\vec{V}u) = D_u \nabla^2 u + A(1-u) - \gamma uv^2, \quad (1)$$

$$\frac{\partial v}{\partial t} + \vec{\nabla} \cdot (\vec{V}v) = D_v \nabla^2 v - Bv + \gamma uv^2, \quad (2)$$

where $\vec{\nabla} = (\partial/\partial x, \partial/\partial y)$, ∇^2 is a two-dimensional (2D) Laplacian, A is the supply rate of u , B is the decay rate of v , and γ is a reaction rate which contains the effect of the global coupling,

$$\gamma = \theta \left(v^* - \int v d^2 r \right), \quad (3)$$

where θ is the Heaviside function and v^* is a parameter representing a threshold of the total amount of v in the system. When the total amount of v becomes larger than v^* , the nonlinear term vanishes and the total amount of v decreases exponentially with the decay rate B . If the feedback were absent, the total amount of v would increase until the pattern filled up the space. Introducing the feedback, we can regulate the total amount of v . We have verified in our simulations that the total amount of v is almost equal to v^* and the deviation from v^* is less than 0.1%.

The velocity field is calculated from a scalar potential,

$$\vec{V} = \vec{\nabla} \phi, \quad (4)$$

$$\nabla^2 \phi = -\alpha v, \quad (5)$$

where we have assumed an irrotational field. The coupling of the reaction and the fluid motion has recently been utilized by Ref. [10] as a model of an electroconvection experiment [11]. Also, some models of chemotactic pattern formation [12] have advection terms and the velocity is determined from the concentration gradient of the chemotactic substance [13,14].

For numerical simulations, we discretized the system into a lattice of 128 by 128 points with each cell size $\Delta x = 1.0$. Fixed boundary conditions ($u=1, v=0$) were adopted. For integrating Eqs. (1) and (2), we employed the explicit Euler method with step size $\Delta t = 0.01$. In each step Eq. (5) was solved by the sine transform with 128×128 bases, according to fixed boundary conditions. These values of Δx and Δt provide good accuracy and efficiency to our calculation, and we have confirmed that using smaller values [$(\Delta x)^2 = 0.1, \Delta t = 0.001$] does not change our results. We take v^* as a con-

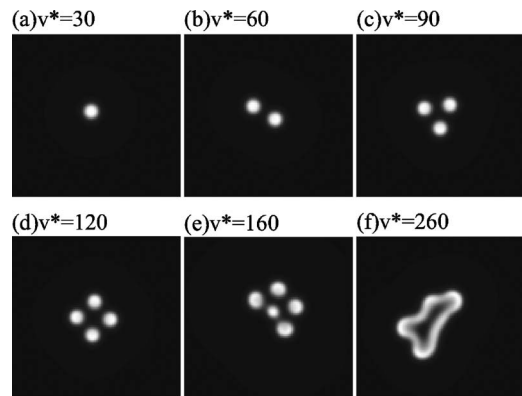


FIG. 1. Snapshots with several values of v^* with $\alpha=0.016$. The v -rich region is represented as white. Only the 100 by 100 region of the entire system is shown. The spots (a)–(e) are in a stationary state, and the loop (f) waves around irregularly.

*Electronic address: yasuaki@daisy.phys.s.u-tokyo.ac.jp

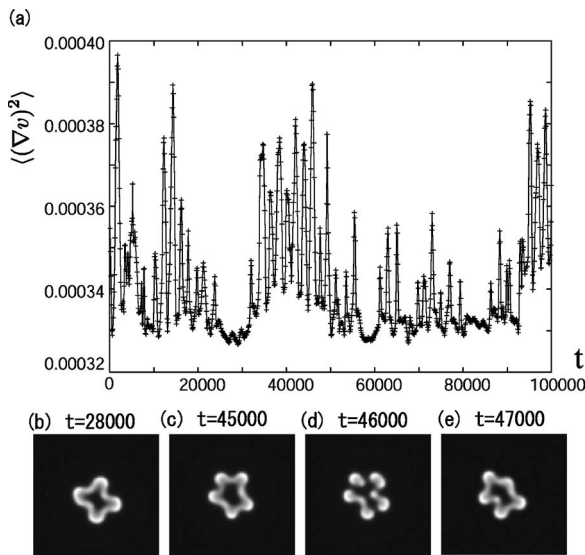


FIG. 2. Time evolution of the wandering loop: $\alpha=0.016$ and $v^*=260$.

control parameter. Unless otherwise noted, we fix the other parameters to the values $D_u=0.2$, $D_v=0.1$, $A=0.025$, $B=0.078$, and $\alpha=0.016$. Later we examine the influence of α and A on the patterns.

Typical patterns for several values of v^* with $\alpha=0.016$ are shown in Fig. 1. The most notable feature is the transition from aggregated spots to a closed loop. The patterns obtained in the simulation have inherited several features from the original Gray-Scott model. For example, a new spot is created by fission of an old spot. However, with fixed v^* , self-replicating dynamics seen in the Gray-Scott model is suppressed by the global constraint of constant $\int v d^2r$. After the fission, the system reaches a stationary state, where the configuration of the spots is highly symmetrical. The number of spots increases as v^* increases. Further increasing v^* , spots

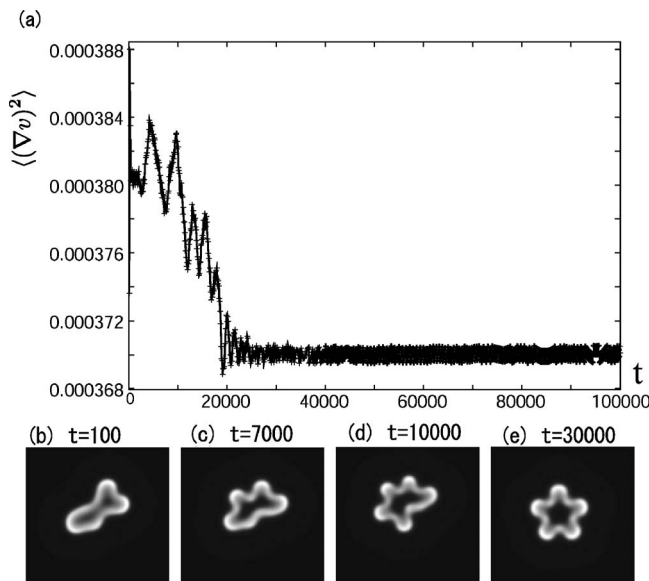


FIG. 3. Dynamics of a loop resulting in a stationary state: $\alpha=0.016$ and $v^*=300$.

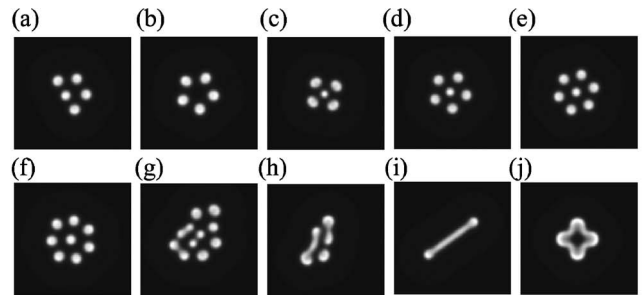
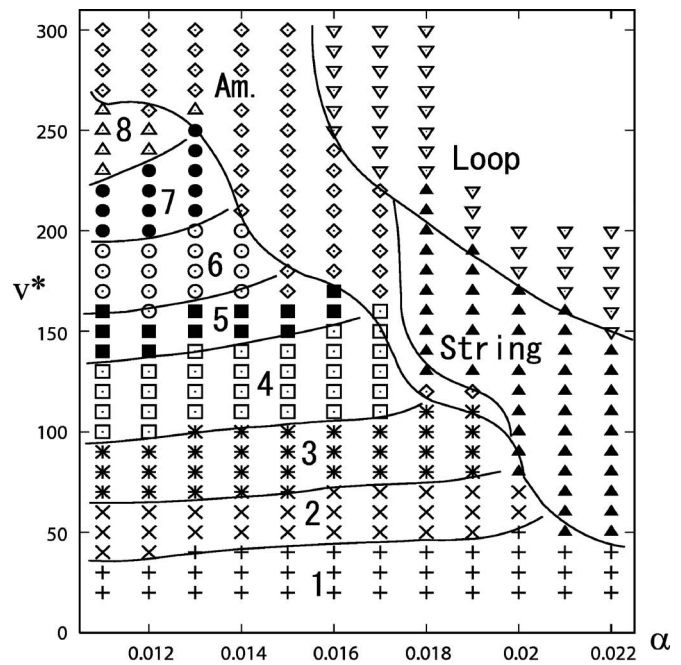


FIG. 4. Phase diagram showing several patterns: one spot (+), two spots (\times), three spots (*), four spots (open square), five spots (closed square), six spots (open circle), seven spots (closed circle), eight spots (open triangle), string (closed triangle), loop (downward open triangle), amorphous state (diamond). Calculations were performed with respect to each column, where the calculation procedure is the same as that in the caption of Fig. 1. (a)–(c): several arrangements of five spots. (a) $\alpha=0.011$, $v^*=150$, (b) $\alpha=0.011$, $v^*=160$, (c) $\alpha=0.013$, $v^*=150$. (d)–(g): Aggregated spots for $\alpha=0.011$ and (d) $v^*=170$, (e) $v^*=200$, (f) $v^*=250$, (g) $v^*=300$. (h) Amorphous state with $\alpha=0.016$, $v^*=210$. (i) and (j) An open string and closed loops with $\alpha=0.018$ and (i) $v^*=150$, (j) $v^*=250$.

become unstable and repeat fusion and fission repeatedly, and at $v^*=250$ a loop is created as shown in Fig. 1(f).

In order to characterize the behavior of the loops, we calculated $\langle (\nabla v)^2 \rangle$, where the brackets $\langle \dots \rangle$ denote the average over the entire space. Although this quantity cannot fully characterize the pattern, it gives us sufficient information on whether a pattern has settled in a stationary state or not. Figure 2 shows the time evolution of the loop. For $v^*=260$, the loop moves around irregularly while changing its shape persistently. Strong bursts reflect the disconnection and reconnection of the loop, which seems to be chaotic. We continued the calculation until $t=10^6$ and found that the pattern was still chaotic. Figure 2(a) can be divided into two periods. In a chaotically bursting period, the shape of the loop is

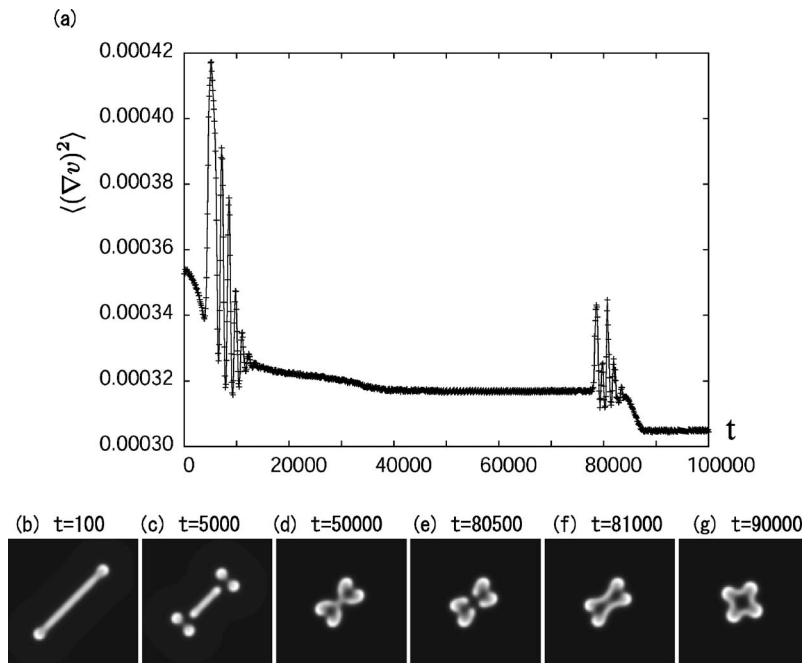


FIG. 5. Collapse of a string into a loop: $\alpha = 0.018$. The initial condition is a stable string with $v^* = 220$, which is increased to $v^* = 230$ at $t = 0$.

basically five-armed as shown in Fig. 2(c), but it is quite unstable and is broken apart as shown in Fig. 2(d). In a calm region such as $t \sim 30\,000$, the loop tends to take four-armed shape as shown in Fig. 2(b), which wanders around without changing its shape. As v^* increases, on the other hand, the loop becomes stable and settles in a stationary state. Figure 3 shows the case of $v^* = 300$. It is clearly seen that the pattern settles in a symmetrical starlike shape by $t = 30\,000$ [15]. Note that the final pattern is similar to Fig. 2(c).

Figure 4 shows the phase diagram in terms of v^* and α . It can be seen from the phase diagram that for α less than 0.015 only aggregated spots can be observed. We have observed only one configuration for each multispot state, except for a five-spot state as shown in Figs. 4(a)–4(c). Two of them [(a) and (b)] belong to the same α with different v^* . There is no hysteresis between (a) and (b). We have observed up to eight stable aggregated spots [Figs. 4(d)–4(f)]. Loop structures arise when α becomes greater than 0.016. There is a wide range of “amorphous state” where the patterns have no definite shapes. For example, we can observe more than eight unstable spots which repeat fusion and fission [Fig. 4(g)]. For α greater than 0.014, the amorphous state comes to consist of spots and strings that also repeat fusion and fission [Fig. 4(h)]. Within our calculation time $t = 10^6$ the amorphous state remained unsteady.

Further increasing α , we can observe a stable string [Fig. 4(i)]. As v^* increases with fixed α , a string suddenly collapses and, through a transient state, turns into a loop [Fig. 4(j)]. The dynamics of the collapse of a string into a loop is shown in Fig. 5. Note that there is a long plateau in (a) which implies a metastable state.

Since our model contains many parameters, we have not yet surveyed the entire parameter space. However, by adjusting other parameters we have found further intriguing dynamics. For instance, with varying A (the supply rate of u), we have observed disappearance and creation of spots. Figure 6 shows the dynamics with $A = 0.017$, $\alpha = 0.01$, and $v^* = 50$.

$= 50$. First a three-spot state loses its stability in an oscillatory manner and one of the spots disappears. Then the remaining spots start to split, and only one of them succeeds to do so, returning to a three-spot state. After an apparently stable three-spot period, spots begin to oscillate and disappear again. The whole process is repeated endlessly. In this case, when v^* increases from $v^* = 20$, we can observe successively one spot, two unstable spots, two stable spots, three unstable spots, and three stable spots. More than three spots are always stable. As A increases with fixed v^* , spots recover their stability. For $A = 0.018$ and other parameters the same, more than two become stable.

One of the important features of the Gray-Scott model is the repulsive interaction of spots; when there are two spots adjacent to each other, the “fuel” u between the spots becomes scarce, which causes further separation. On the other hand, the advection terms induce attractive interaction due to the velocity field created by v . Since the flow is canceled out between the spots, the entire flow makes the spots move toward one another. So there exists a long-range attraction and a short-range repulsion between spots, and competition between them is responsible for the transition to loops.

The transition presented here is quite similar to one observed by Nasuno in a gas-discharge experiment [16], where luminous discharge regions between two electrodes form localized patterns which undergo a transition from a cluster of spots through an open string to a waving loop. Furthermore, disappearance and reproduction of spots as shown in Fig. 6

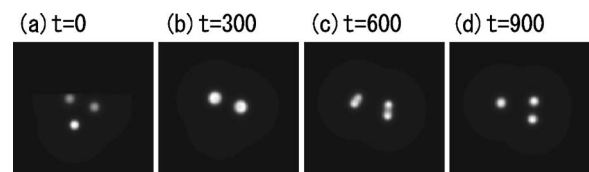


FIG. 6. Disappearance and reproduction of spots: $A = 0.017$, $\alpha = 0.01$, and $v^* = 50$.

are also observed in Nasuno's experiment. This similarity encourages us to interpret our system as a model of Nasuno's experiment. In the context of Nasuno's system, u and v are regarded as the concentration of some species that comprises the air and its ionized state, respectively. Existence of the global coupling term corresponds to the fact that the experiment was performed under the condition of constant current, which implies a constant discharge area. Also, the velocity field might be caused by discharge flows. Discharge flows perpendicular to the electrodes induce the flows parallel to them. Then ϕ in Eq. (5) can be interpreted as a two-dimensional velocity potential.

Even if our model can be interpreted as a model of Nasuno's system, so far we have failed to observe some intriguing behavior which has also been observed in Nasuno's experiment. For instance, in Nasuno's experiment spots sometimes change their configuration with lowering the symmetry, with all the parameters fixed. In contrast, in our model, a cluster of spots takes several forms in a transient period but finally reaches a stationary state which has higher symmetry than the transient form has, except in the case of a loop state as in Fig. 2, where we can observe chaotic transition of patterns.

There are other models describing clusters of spots in reaction-diffusion systems [6,8]. But the mechanism of cre-

ating clusters of spots in these models is different from ours. In these models, interaction of two spots is oscillatory; the force between them changes its sign periodically as increasing the distance between the spots. As a consequence, spots take limited configurations where spots are put on a triangular lattice. On the other hand, as stated above, in our model reaction terms are repulsive, and the velocity field is responsible for attractive interaction. This means that there is no limitation that confines the spots on a lattice. Thus we have, for example, a square configuration as shown in Fig. 1(d) and others shown in Fig. 4. We should mention that Nasuno's experiment also shows such square and other configurations. A plausible reason of the difference between the experiments described by these models [6,8] and Nasuno's is that the former used semiconductor as electrodes, as opposed to metal in the latter. Using metal makes us unable to choose the potential drop as one of the variables as Refs. [6,8]. So our work is not incompatible with these models.

We thank H. Wada and Y. Murayama for useful discussions. This work was supported by a Japanese Grant-in-Aid for Scientific Research from the Ministry of Education, Science, Sports, and Culture of Japan (Contract No. 16206020).

-
- [1] P. B. Umbanhowar, F. Melo, and H. L. Swinney, *Nature (London)* **382**, 793 (1996).
 - [2] A. Joets and R. Ribotta, *Phys. Rev. Lett.* **60**, 2164 (1988).
 - [3] K. Lerman, E. Bodenschatz, D. S. Cannell, and G. Ahlers, *Phys. Rev. Lett.* **70**, 3572 (1993).
 - [4] O. Lioubashevski, H. Arbell, and J. Fineberg, *Phys. Rev. Lett.* **76**, 3959 (1996); O. Lioubashevski, Y. Hamiel, A. Agnon, Z. Reches, and J. Fineberg, *Phys. Rev. Lett.* **83**, 3190 (1999).
 - [5] E. Ammelt, D. Schweng, and H.-G. Purwins, *Phys. Lett. A* **179**, 348 (1993).
 - [6] Yu. A. Astrov and Yu. A. Logvin, *Phys. Rev. Lett.* **79**, 2983 (1997).
 - [7] B. Schäpers, M. Feldmann, T. Ackemann, and W. Lange, *Phys. Rev. Lett.* **85**, 748 (2000).
 - [8] C. P. Schenk, P. Schütz, M. Bode, and H.-G. Purwins, *Phys. Rev. E* **57**, 6480 (1998).
 - [9] P. Gray and S. K. Scott, *Chem. Eng. Sci.* **38**, 29 (1983); P. Gray and S. K. Scott, *Chem. Eng. Sci.* **39**, 1087 (1984).
 - [10] I. S. Aranson and M. V. Sapozhnikov, *Phys. Rev. Lett.* **92**, 234301 (2004).
 - [11] M. V. Sapozhnikov, Y. V. Tolmachev, I. S. Aranson, and W.-K. Kwok, *Phys. Rev. Lett.* **90**, 114301 (2003).
 - [12] E. O. Budrene and H. C. Berg, *Nature (London)* **349**, 630 (1991); E. O. Budrene and H. C. Berg, *Nature (London)* **376**, 49 (1995).
 - [13] E. F. Keller and L. A. Segel, *J. Theor. Biol.* **26**, 399 (1970).
 - [14] M. Mimura and T. Tsujikawa, *Physica A* **230**, 499 (1996).
 - [15] The jittering of the graph in Figs. 2 and 3 after reaching the stationary state is due to the Heaviside function and can be removed by using a smooth function such as tanh without changing any qualitative feature.
 - [16] S. Nasuno, *Chaos* **13**, 1010 (2003).